FACETS
a multidisciplinary open access science journal

RESEARCH ARTICLE

Using Holocene paleo-fire records to estimate carbon stock vulnerabilities in Hudson Bay Lowlands peatlands

M.A. Davies[ab*†] J.W. McLaughlin[b], M.S. Packalen[b], and S.A. Finkelstein[a*]

[a]Department of Earth Sciences, University of Toronto, 22 Ursula Franklin Street, Toronto, ON M5S 3B1, Canada; [b]Ontario Forest Research Institute, Ministry of Northern Development, Mines, Natural Resources and Forestry, 1235 Queen Street E, Sault Ste. Marie, ON P6A 2E5, Canada

*m3davies@uwaterloo.ca; sarah.finkelstein@utoronto.ca
[†]Present address: Department of Geography and Environmental Management, 200 University Avenue W, University of Waterloo, Waterloo, Ontario, N2L 3G1, Canada.

Abstract

Holocene fire records from charcoal are critical to understand linkages between regional climate and fire regime and to create effective fire management plans. The Hudson Bay Lowlands (HBL) of Canada is one of the largest continuous peatland complexes in the world and is predicted to be increasingly impacted by wildfire. We present three charcoal records from a bog in the western HBL and demonstrate that median fire frequency was higher in the Middle Holocene, related to warmer regional temperatures and higher evaporative demand. Holocene fire frequencies are lower than in western Canadian peatlands, supporting that the HBL lies in the transition between continental and humid boreal fire regimes. Apparent carbon accumulation rates at the site were not significantly different between the Middle and Late Holocene, suggesting that higher fire frequency and enhanced decomposition offset the potential for higher rates of biomass production. We compile records from the boreal region and demonstrate that increasing fire frequency is significantly correlated with diminishing long-term carbon accumulation rates, despite large variation in response of peatlands to fire frequency changes. Therefore, the paleo-record supports that higher fire frequencies will likely weaken the capacity of some northern peatlands to be net carbon sinks in the future.

Key words: peatland, Hudson Bay Lowlands, charcoal, fire, Holocene, soil carbon accumulation

Citation: Davies MA, McLaughlin JW, Packalen MS, and Finkelstein SA. 2023. Using Holocene paleo-fire records to estimate carbon stock vulnerabilities in Hudson Bay Lowlands peatlands. FACETS 8: 1–26. doi:10.1139/facets-2022-0162

Handling Editor: Clément pierre Bataille

Received: July 14, 2022

Accepted: September 23, 2022

Published: February 2, 2023

Published by: Canadian Science Publishing

1. Introduction

Peatlands are a type of wetland ecosystem where significant organic matter accumulates under anoxic and waterlogged conditions. As a result, these ecosystems store a third or more of the soil carbon pool (Gorham 1991; Yu et al. 2010; Nichols and Peteet 2019). Although these ecosystems have been net carbon sinks over Holocene timescales, the relative roles of carbon uptake and release remain uncertain with anthropogenic climate change, particularly in the context of disturbances such as fire (Gallego-Sala et al. 2018; Loisel et al. 2021).

Fire directly impacts peatland carbon cycling through the combustion of surface vegetation and peat, which releases carbon dioxide, carbon monoxide, methane, and other hydrocarbons to the atmosphere (Kasischke and Bruhwiler 2002; Turetsky et al. 2002). In northern regions, peatland ecosystems can be resilient to fire through rapid vegetation recovery (on the order of decades;

Wieder et al. 2009; Lukenbach et al. 2015a; Hokanson et al. 2016; Ingram et al. 2019) and the stabilization of organic matter during combustion (Heinemeyer et al. 2018; Flanagan et al. 2020; Pellegrini et al. 2021). However, under regional climates that promote high fire frequency and prolonged summer drought, northern peatlands can become net sources of carbon, especially when sites are prone to water table drawdown (Wieder et al. 2009; Ingram et al. 2019). In Canada, fire frequency and spreading days are already increasing across the boreal biome and this trend is expected to continue (Kasischke and Turetsky 2006; Wang et al. 2017). These increases are expected to be especially pronounced in the western boreal region, where high fire frequency and large burned area annually already occur (Kasischke and Turetsky 2006; Wang et al. 2017; Erni et al. 2019). Furthermore, summer evapotranspiration is expected to outpace precipitation increases in northern and central Canada (Tam et al. 2019) and in peatland ecosystems, a stronger response to changing vapor pressure deficits with warming than adjacent forests means evaporation losses from the boreal region could be underestimated (Helbig et al. 2020). Higher summer water deficits in boreal Canada will likely result in larger lags in post-fire recovery of peatlands, expose deeper peats to potential combustion, and make more peatlands vulnerable to fire depending on local hydrological and climatic factors (Lukenbach et al. 2015b; Turetsky et al. 2015). Therefore, constraining spatial and temporal variability in peatland response to changing fire regimes is critical to make impactful fire management decisions (Flannigan et al. 2009; Ingram et al. 2019) and to quantify the future strength of the peatland carbon sink in the 21st century and beyond (Loisel et al. 2021; Müller and Joos 2021).

Reconstructing long-term changes in peatland fire regimes of the past allows for baseline data on long-term fire frequency, which can be linked to past climates and inform future scenarios. In North America, fire frequency also differed between western and eastern boreal regions across the Holocene due to spatial variability in paleoclimatic change (Kuhry 1994; Carcaillet and Richard 2000; van Bellen et al. 2012). In the relatively warmer and drier conditions of the Middle Holocene, western boreal regions in North America experienced higher fire frequency compared to the Late Holocene (northern Alberta; Kuhry 1994; Zoltai et al. 1998). As a result, peatlands that experienced fire generally accumulated less carbon, despite warm conditions and longer growing seasons promoting peat growth and higher carbon accumulation rates globally (Kuhry 1994; Loisel et al. 2014). In the eastern boreal region of North America, higher humidity and fewer incursions of dry Pacific air masses meant lower Middle Holocene fire frequencies compared to the Late Holocene, and therefore, fire played less of a role in peatland carbon cycling (northern Quebec; Carcaillet and Richard 2000; van Bellen et al. 2012). However, responses to regional climatic changes are site specific, as successional stages and hydrological conditions can prevent fire and mitigate against carbon loss (Camill et al. 2009; Magnan et al. 2012). Therefore, local factors and how they change through time need to be constrained to determine whether changes in the fire record at a peatland site are reflective of regional climatic conditions.

The Hudson Bay Lowlands (HBL) has not been as well studied in terms of impacts of fire on peatland carbon storage across Holocene timescales, despite fire occurring on the modern landscape (**Fig. 1**; Stocks et al. 2002; Coops et al. 2018) and the need to include how fire frequency change in response to drier relative conditions will impact the carbon sink capacity of this large peatland complex in the future (Chaudhary et al. 2020; Qiu et al. 2020; McLaughlin and Packalen 2021; Qiu et al. 2022). The modern fire return interval (FRI) for the HBL region is estimated to be between 400 and 900 years based on historical records of burned area and is more similar to eastern (300–700 years) than western (100–400 years) boreal fire occurrence (Stocks et al. 2002; Coops et al. 2018). The burned area pattern across the HBL is, however, not uniform, with more area burned along the western margin near the Boreal Shield (**Fig. 1**; Canadian Forest Service 2020; Hall et al. 2020). The HBL also lies between the western and eastern boreal fire patterns documented across the

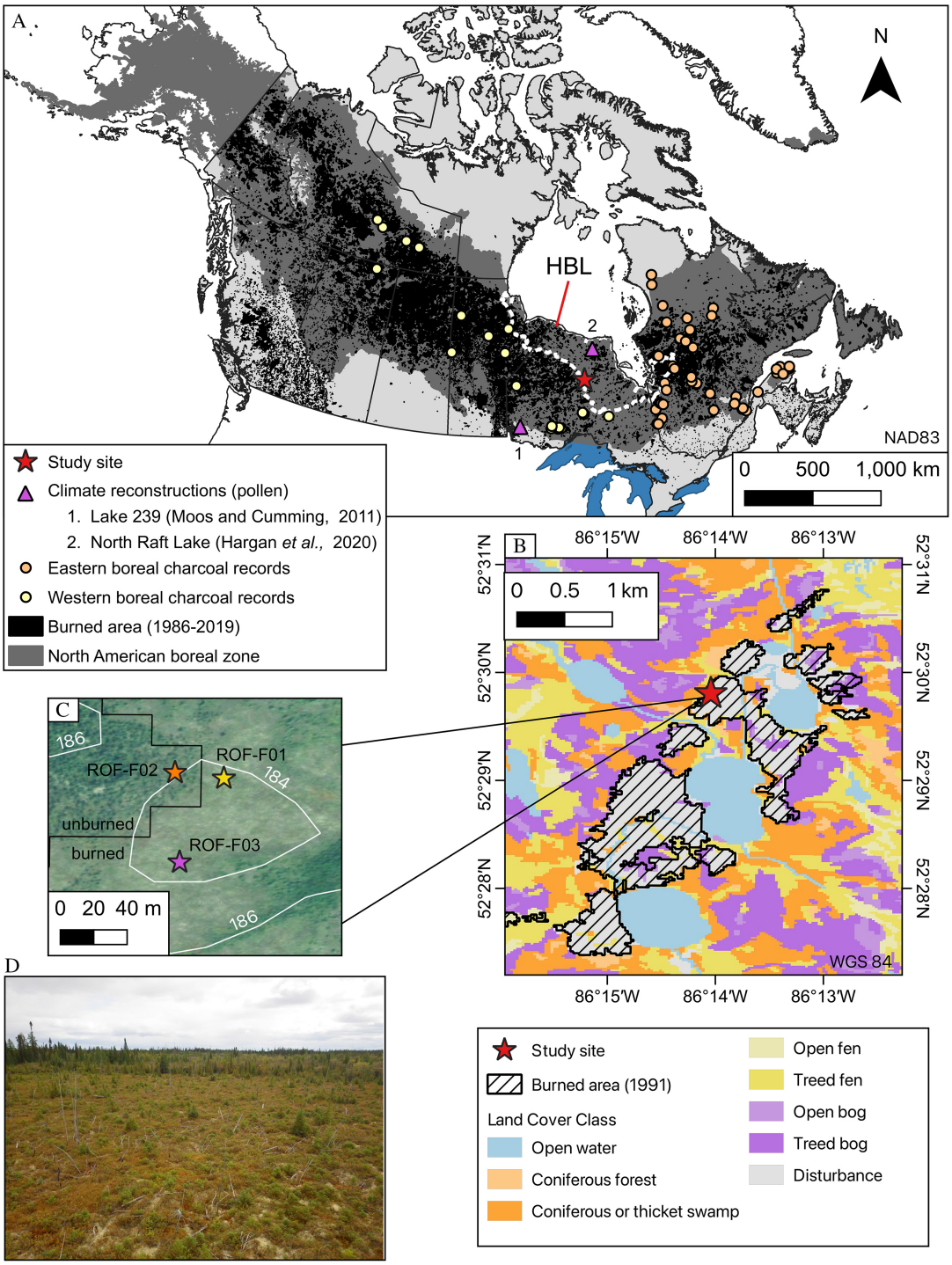

Fig. 1. Map and image of the study site and coring localities in the western Hudson Bay Lowlands (HBL), Canada. (A) Map of North America, showing the boreal zone (after Brandt 2009), the HBL region (after the Hudson Plains Ecozone of Ecological Stratification Working Group1995), and burned area in Canada from 1986 to 2019 (Canadian Forest Service 2020; Hall et al. 2020). Circles show the locality of lake charcoal records from the Global Charcoal Database (Power et al. 2010) used to create western and eastern fire history curves found in **Fig. 6**. Individual site information and references are found in **Tables S1** and **S2**. Star shows the study site and triangles show lake records found in **Fig. 6**. (B) Map showing the 1991 fire areal extent (Canadian Forest Service 2020; Hall et al. 2020) and land cover classes (Government of Ontario 2021). (C) Map showing the coring locations within the study site. Labeled white lines are elevation, in meters. Imaging from Google Earth. (D) Image of the study site, facing west. Photo credit: M. Davies.

Holocene in previous studies (e.g., Kuhry 1994; Camill et al. 2009; van Bellen et al. 2012) and could therefore record a different pattern of fire frequency changes, depending on the location within the HBL. Therefore, charcoal records are needed to constrain paleo-fire frequency and determine the response of HBL peatland fire regimes to past climates to support the inclusion of fire into modeled predictions of future carbon uptake and loss for the region.

Here, we present three paleo-fire records from a site on the western margin of the HBL. The study has three major goals: (1) to compare the site's Holocene fire frequency patterns to both compilations of lake sediment charcoal records and other peatland sites from Canada to investigate how the study region compares to western and eastern boreal fire frequency patterns through pre-industrial climatic changes of the Holocene, (2) to investigate the role of fire on carbon accumulation rates and calculate the potential carbon loss resulting from changing fire frequency at the site, and (3) to determine a relationship between fire frequency and carbon accumulation by combining our site's records with data from other boreal peatland sites outside the HBL region.

2. Methods

2.1. Study region and sampling

The study site is located on the western margin of the HBL, Canada (**Fig. 1**; the Hudson Plains Ecozone of the Ecological Stratification Working Group 1995). The study site and surrounding area are underlain by Paleozoic carbonates, shales, and siltstones and are close to the boundary with the Archean Superior Province of the Canadian Shield (Ontario Geological Survey 2011). Surficial deposits consist of peat and massive to bedded diamicton (Barnett et al. 2013a; 2013b). Land coverage is almost entirely peatlands and other wetlands, with minor extent of coniferous forest in slight upland regions (**Fig. 1**; Government of Ontario 2021). Peat depth is generally shallow in the area immediately surrounding the study site, ranging from 100 to 150 cm.

The HBL has a humid microthermal Arctic climate (Martini 2006). Mean annual temperature is −1.3 °C and total annual precipitation is 700 mm at the closest weather station (Lansdowne House; approximately 120 km from the study site; Government of Canada 2021). The highest and lowest average monthly temperatures occur in July and January, respectively (17.2 °C and −22.3 °C). Snowfall >20 cm occurs in 7 months of the year (October to April; 242 cm yr^{-1} total; Government of Canada 2021).

The study site was accessed by helicopter and is located within the northwestern portion of an area that burned in the summer of 1991 (**Fig. 1**; identified via satellite imagery [Landsat]; Canadian Forest Service 2020; Hall et al. 2020). The fire was caused by lightning and an estimated 76–100% of the delineated area in **Fig. 1** was burned (420 Ha; Canadian Forest Service 2020; Hall et al. 2020). The burned portion of the study site is a shrub-rich bog with hummock and hollow microtopography and is predominantly surrounded by unburned forested bog (**Fig. 1**). Vegetation consisted of predominantly *Picea mariana*, *Rhododendron groenlandicum*, and *Sphagnum* and *Cladina* spp. in both the burned and unburned portions of the study site. *Chamaedaphne calyculata*, *Maianthemum trifolium*, and *Rubus chamaemorus* were also present. *Eriophorum vaginatum* and *Larix laricina* were also found infrequently surrounding each of the coring localities. Water table depth and pH were measured at two points at the site at the time of sampling (hollow and high hummock) and were 42 and 66 cm and 5.0 and 3.6, respectively. Three cores were collected in August 2018 at the study site, "ROF-F01," "ROF-F02," and "ROF-F03" (184 m asl; **Fig. 1**; **Table 1**). The cores were taken in different regions of the site (burned-edge, burned-center, unburned) and in different microtopography (low hummock, hollow, high hummock) to capture some of the spatial variability (**Table 1**). Coring was done using a 1-m Jeglum corer for the first 100 cm; subsequent drives were collected with a

Table 1. Summary information, Holocene fire patterns, and carbon release and storage for ROF-F01, ROF-F02, and ROF-F03. Center and edge refer to the locality within the 1991 burned area of the study site. Potential carbon loss is estimated by assuming 1430 g C m^{-2}·yr^{-1}·$fire^{-1}$ after Balshi et al. (2009) for the Hudson Plains. FRI: fire return interval; freq.: frequency; LORCA: long-term rates of carbon accumulation, equal to the total carbon mass divided by the basal age; SNI: signal-to-noise index.

Core	ROF-F01		ROF-F02	ROF-F03
A. Site information				
Latitude (°N)	52.4967		52.4968	52.4960
Longitude (°W)	86.2336		86.2340	86.2340
Microtopography at core location	Low hummock		Hollow	High hummock
Location description	Burned-edge		Unburned	Burned-center
Basal peat depth (cm)	91		130	135
Basal age (cal yr BP)	6500		5600	7200
B. CharAnalysis inputs and Holocene fire patterns				
Core interval	A	B	—	—
Age interval	0–440	2900–6500	—	—
Charcoal median sampling resolution (yrs)	17	73	55	38
Smoothing window (yrs)	500	2200	1700	1200
Threshold	Global	Local	Local	local
Median SNI	45.6	13.0	12.9	6.5
Samples SNI >3	—	51/51	104/104	167/196
Number of peaks	2	3	5	9
Number of fires	6		5	9
Number of peaks with smoldering evidence	4		3	3
Number of FRI	4		4	8
Mean Holocene FRI (yr·$fire^{-1}$)	930		990	907
Mean Holocene fire freq. (# 1000 yr^{-1})	1.1		1.0	1.1
C. Mean peat properties and net carbon accumulation and release estimates				
Mean C content (± SD; %)	46 ± 4		44 ± 3	43 ± 4
Mean N content (± SD; %)	0.8 ± 0.3		0.7 ± 0.2	1.0 ± 0.3
Mean C:N ratio (± SD)	64 ± 20		69 ± 19	49 ± 14
Mean carbon density (± SD; kg C m^{-3})	57 ± 32		47 ± 23	55 ± 22
Total carbon mass (kg C m^{-2})	53		60	76
LORCA (g C m^{-2}·yr^{-1})	8.1		10.8	10.3
Holocene carbon loss from fire (kg C m^{-2})	10		8	11

1 m × 15 cm diameter Russian peat corer. Basal sediments underneath the peat at each coring locality consisted of a clay matrix and grains of silt and sand. Cores were stored at 4 °C prior to analysis at the University of Toronto, Canada.

2.2. Chronology and peat properties

The approach for sampling for chronology and peat properties was the same for each coring locality, with exceptions noted below. Ages were assigned to each core using Bayesian age-depth modeling in the "rbacon" package for R (Blaauw and Christen 2011). Each model was developed using radiocarbon dates on aboveground plant material (**Table 2**) and the surface age (−68 cal yr BP). A total of seven to nine radiocarbon dates per core were measured to obtain a resolution of roughly one date per 1000 years. Cores were initially dated at 45 cm, 95 cm, and the base of the core, and additional dates between these were measured to obtain the targeted resolution. Conventional ^{14}C ages were calibrated to "calendar" (cal) years using the IntCal20 calibration curve (Reimer et al. 2020). Radiocarbon ages were measured at the Lalonde AMS Laboratory (Ottawa, Canada). For the coring locality adjacent to the burned area (ROF-F02), where there was no suspected disturbance of the upper peat column from the most recent known fire, Pb-210 activities from bulk peat samples in the upper 50 cm were also used in the Bayesian age-depth model for the location using the "plum" package for R (**Table 3** and **Fig. S1**; Blaauw et al. 2021). Pb-210 samples were measured at the Flett Research Laboratory using alpha spectrometry (Winnipeg, Canada). Select samples across the upper 50 cm of the core were measured to obtain sufficient data to determine exponential decrease in Pb-210 activity to background levels (**Table 3** and **Fig. S1**). Because the coring locality had Pb-210 ages, radiocarbon ages above 45 cm were not measured. We placed a hiatus in a record when the average accumulation rate between radiocarbon ages was much lower than our prior accumulation rate in our Bayesian age-depth model (i.e., << 50 years·cm^{-1}; threshold of 5 × lower = 250 years cm^{-1}).

To estimate long-term and apparent carbon accumulation rates (aCARs), carbon density, and total carbon mass, and to investigate peat properties (carbon and nitrogen content), dry bulk density measurements were performed at a 1 cm resolution to match the highest resolution of the charcoal record. A total of 2–28 cm^3 was taken from each 1 cm interval to obtain >0.5 g of the dried sample for carbon and nitrogen analysis. Each sample was dried to a constant mass overnight at 60 °C and then ground to a fine powder using a MM200 Retch ball mill. Carbon and nitrogen analysis was performed at the Radiochronology Lab at the Centre for Northern Studies, Université Laval (Québec City, Canada), where 70–100 mg per sample was analyzed using a Leco CHN628 analyzer. Standards analyzed alongside samples were within 0.6% relative standard deviation for both carbon and nitrogen (EDTA Lot1061 and 502-309 soil standard). Carbon accumulation rates were calculated using two methods, aCARs and long-term rates of carbon accumulation (LORCAs). LORCAs represent the net carbon storage at the site through its averaged accumulation history, while aCARs are time-stepped estimates approximating net carbon uptake at a given time (Young et al. 2021). aCARs were calculated by multiplying the dry bulk density (in g cm^{-3}) by the accumulation rate (cm yr^{-1}) and the proportion of carbon in each sample (Chambers et al. 2010). Cumulative carbon mass was determined by summing the carbon densities (in kg C m^{-3}) multiplied by the thickness (in m) for each sample. The cumulative carbon mass (in kg C m^{-2}) was then used to calculate LORCA for each coring locality by dividing it by the basal age.

2.3. Charcoal and peat type analysis

To assess fire frequency through the Holocene, subsamples of 2 cm^3 of peat were taken contiguously along each core at a 1–2 cm interval. Each sample was placed in a 5% KOH treatment overnight (>16 h) and then sieved to >150 µm (after Mooney and Tinner 2010; van Bellen et al. 2012). The entire sample was counted using a stereomicroscope with a gridded Petri dish at 32 × magnification.

Table 2. AMS radiocarbon ages for ROF-F01, ROF-F02, and ROF-F03, western Hudson Bay Lowlands, Canada. Individual age calibrations in this table were performed using OxCal version 4.4 (Bronk Ramsey 2009).

Depth (cm)	Radiocarbon age (^{14}C yr. BP)	Material	Cal BP (2σ range)	Lab ID
A. ROF-F01				
15–16	> modern F^{14}C: 1.7387 ± 0.0058	*Sphagnum* stems and leaves	1963–1966 (95.4%) AD	UOC-14867
35–36	79 ± 26	*Sphagnum* stems and leaves Conifer needles	257–224 (26.5%) 140–32 (69.0%)	UOC-14868
25–26	154 ± 27	*Sphagnum* stems and leaves	284–240 (16.3%) 233–167 (28.7%) 155–128 (9.9%) 119–57 (21.1%) >45 (19.4%)	UOC-13269
45–46	158 ± 25	*Sphagnum* stems and leaves	285–246 (16.3%) 230–166 (32.6%) 157–133 (9.8%) 118–59 (20.4%) >44 (20.4%)	UOC-13270
55–56	2929 ± 27	*Sphagnum* stems and leaves	3167–2994 (93.1%) 2980–2968 (2.3%)	UOC-14869
65–66	2625 ± 29	*Sphagnum* stems and leaves	2776–2723 (95.4%)	UOC-13271
72–73	4142 ± 27	*Sphagnum* stems and leaves	4824–4743 (30.8%) 4736–4572 (64.2%) 4540–4537 (0.4%)	UOC-14870
80–81	4755 ± 31	*Sphagnum* stems and leaves	5584–5457 (83.9%) 5378–5330 (11.6%)	UOC-13272
91–92	5719±30	*Sphagnum* stems and leaves Ligneous fragments	6266–6581 (10.4%) 6569 (80.7%) 6425–6407 (4.4%)	UOC-13273
B. ROF-F02				
45–46	302 ± 28	*Sphagnum* stems and leaves	455–348 (70.5%) 340–296 (24.9%)	UOC-13274
70–71	632 ± 27	*Sphagnum* stems and leaves	659–533(95.4%)	UOC-13275
80–81	1737 ± 27	*Sphagnum* stems and leaves	1703–1549 (95.4%)	UOC-14871
95–96	2616 ± 29	*Sphagnum* stems and leaves	2771–2721 (95.4%)	UOC-13276
115–116	4442 ± 27	*Sphagnum* stems and leaves Conifer needles Brown moss stems	5280–5166 (35.2%) 5137–5100 (7.5%) 5081–4958 (47.8%) 4932–4883 (5.0%)	UOC-14872
120–121	4320 ± 29	*Sphagnum* stems and leaves Conifer needles	4960–4840 (95.4%)	UOC-13277
128–129	4830 ± 33	*Sphagnum* stems and leaves	5601–5476 (95.4%)	UOC-13278
C. ROF-F03				
25–26	88 ± 26	*Sphagnum* stems/leaves	260–222 (26%) 142–30(69.4%)	UOC-14873

(*continued*)

Table 2. (*concluded*)

Depth (cm)	Radiocarbon age (^{14}C yr. BP)	Material	Cal BP (2σ range)	Lab ID
45–46	290 ± 26	*Sphagnum* stems/leaves	445–354 (63.7%) 334–290 (31.7%)	UOC-13280
60–61	1468 ± 28	*Sphagnum* stems/leaves	1387–1304 (95.4%)	UOC-14874
70–71	1769 ± 26	*Sphagnum* stems/ leaves + conifer needles	1719–1588 (95.4%)	UOC-13281
80–81	2439 ± 25	Ligneous fragments conifer needles *Sphagnum* stems/leaves	2699–2635 (21.4%) 2616–2587 (8.9%) 2537–2529 (0.8%) 2520–2357 (64.3%)	UOC-14875
95–96	2895 ± 26	Conifer needles/*Sphagnum* stems/leaves	3152–3090 (13.0%) 3082–2952 (82.5%)	UOC-13281
115–116	5041 ± 27	Ligneous fragments/ *Sphagnum* stems and leaves conifer needles	5900–5716 (94.6%) 5671–5665 (0.9%)	UOC-14876
125–126	5815 ± 34	*Sphagnum* stems/leaves ligneous fragments	6730–6699 (5.7%) 6678–6499 (89.7%)	UOC-13282
134–135	6277 ± 36	*Sphagnum* stems/leaves ligneous fragments	7280–7155 (88.0%) 7118–7066 (5.4%) 7049–7024 (2.0%)	UOC-13283

Charcoal fragments were identified by referencing New et al. (2016) (**Fig. S2**). Peat type was assigned to each sample based on the main vegetation groups observed. Samples were assigned to one of three groups: *Sphagnum*-dominated peat, mixed ligneous and *Sphagnum* peat, and mixed ligneous, *Sphagnum*, and herbaceous peat. To be assigned a group, each of the various plant macrofossil components was at least 25% of the plant macrofossils present in the sample.

2.4. Fire identification

Charcoal counts were analyzed to identify fire peaks using "CharAnalysis" (Higuera 2009). Each core was rescaled to the median sample resolution prior to analysis to reduce bias from a changing vertical accretion rate in the site's accumulation history (**Table 1**). If a core had a suspected hiatus, it was split into two components (i.e., above and below the boundary; Section A and B; **Table 1**). The rescaled charcoal accumulation rate (CHAR) was split into three components: background (C_{back}), noise (C_{noise}), and fire (C_{fire}). The background component is attributed to changes in long-term regional charcoal production and transport, post-fire deposition, and the potential movement of charcoal within the acrotelm (Higuera et al. 2009; van Bellen et al. 2012). Both the noise and fire components are part of the peaks (C_{peak}) identified above C_{back}, where C_{noise} is attributed to random variability due to external inputs, and the C_{fire} represents charcoal produced due to local burning at or near the site (Gavin et al. 2006; Higuera et al. 2010). We defined C_{peak} as a residual, assuming that there is an additive relationship. We identified C_{back} using LOWESS smoothing (robust to outliers) and defined the smoothing window to have >30 samples per window (Higuera et al. 2010). We used a local threshold to separate C_{fire} and C_{noise} to account for variation in the record with decomposition when the core intervals analyzed were greater than the smoothing window (**Table 1**; Higuera et al. 2010). C_{fire} was considered to represent a local peat fire when it was above the 99% threshold of the C_{noise} distribution identified using Gaussian mixture models (Gavin et al. 2006). We utilized a signal-to-noise index

Table 3. Pb-210 activity for ROF-F02, western Hudson Bay Lowlands, Canada. Lower three samples were used for supported activity calculations. SD: standard deviation; DPM: disintegrations per minute; 0.06 DPM·g^{-1} = 1 Becquerel (Bq)·kg^{-1}.

Interval (cm)	^{210}Pb total activity (DPM·g^{-1})	^{210}Pb total activity SD (DPM·g^{-1})	Bulk density (g cm^{-3})
0–1	21.27	0.54	0.036
2–3	33.02	0.75	0.035
3–4	31.81	0.63	0.074
5–6	25.32	0.57	0.068
6–7	23.74	0.52	0.065
7–8	24.23	0.58	0.046
9–10	11.53	0.43	0.054
10–11	6.89	0.32	0.061
12–13	4.09	0.24	0.055
14–15	3.04	0.20	0.046
16–17	2.46	0.20	0.054
24–25	2.20	0.19	0.064
29–30	1.57	0.15	0.075
34–35	0.89	0.10	0.055
39–40	0.25	0.07	0.070
44–45	0.01	0.04	0.080
49–50	0.06	0.04	0.085

(SNI) to evaluate each of the peaks in our record (after Kelly et al. 2011). A SNI greater than 3 for a given peak was the threshold to consider a peak well separated from C_{noise}. To separate peaks that directly impacted the peat column and those that impacted vegetation inputs, we used C:N ratio, as N is enriched relative to C during peat smoldering (Zaccone et al. 2014).

2.5. Local and regional fire frequency and carbon accumulation

Relationships between FRI and aCAR through the Holocene were investigated using the combined datasets of the three coring localities. FRI and aCAR values were assigned to one of the following intervals: 0–500 cal yr BP, 500–4200 cal yr BP, and 4200–7200 cal yr BP. We selected 500 cal yr BP as a boundary because aCARs shift to much higher values associated with acrotelm peat that cannot be directly compared to deeper values (Young et al. 2019). Further, there could be potentially higher amounts of charcoal movement through fluctuating water tables in acrotelm peat. Therefore, these values were omitted from the statistical analysis of the difference between aCAR values through time and their relation to changing FRIs. The boundary between the other two intervals is the stage boundary between the Middle and Late Holocene (4200 cal yr BP; Walker et al. 2019). For FRIs that overlapped the boundaries, they were assigned to the interval where the majority of the FRI occurred. A Mann–Whitney U test was performed to test differences between aCARs between the Middle (4200–7400 cal yr BP; N = 74, 3 coring locations) and Late Holocene (500–4200 cal yr BP N = 123, 3 coring locations). This test was selected because the aCAR data are non-normal (Shapiro–Wilk, $p < 0.05$). Statistical tests were not performed on the FRI data, as sample size for each interval was

low, even in the combined record. Median fire frequency values were used in the comparison between time periods to minimize the influence of outliers. We estimated carbon release for the Middle and Late Holocene time bins (in kg C m^{-2}) by multiplying the median fire frequency (1/FRI; in fires·yr^{-1}) and time bin interval (yr) by the annual average emission per unit of burned area within the Hudson Plains (1430 g C m^{-2}·$fire^{-1}$; Balshi et al. 2009). This annual average emission value was selected as it is a modeled estimate for the entire region and also lies conservatively within estimates of carbon loss from fire in boreal peatlands, which is expected in more humid regional climates such as the HBL where fire is more likely restricted to aboveground biomass (0–6000 g C m^{-2}·$fire^{-1}$; Zoltai et al. 1998; Turetsky and Wieder 2001; Lukenbach et al. 2015b; Wilkinson et al. 2018).

Holocene-scale fire frequencies were used to place our study region in the wider context of the relationship between fire frequency and LORCAs in peatlands across the boreal region. A Holocene-scale fire frequency (in fires 1000·yr^{-1}) was calculated for each coring location by dividing the total number of fire peaks by the basal age. A Holocene FRI was then calculated as the inverse of fire frequency. We estimated carbon release at each coring location for the entire record (in kg C m^{-2}) by multiplying the median fire frequency (1/FRI; in fires·yr^{-1}) and the core basal age (yr) by the annual average emission per unit of burned area within the Hudson Plains as above (1430 g C m^{-2}; Balshi et al. 2009). To compare our study site to other boreal regions, we compiled fire frequency and LORCA data from other boreal peatlands (Kuhry 1994; Turunen et al. 2001; van Bellen et al. 2012; Magnan et al. 2020) and investigated their relationship using linear regression analysis. A linear relationship was explored as this was previously found to be significant (Kuhry 1994; Moore and Robinson 2000). Fire frequency was square-root transformed prior to linear regression analysis to normalize the dataset (Shapiro–Wilk, $p > 0.05$).

We utilized the "Global Charcoal Database" to create compilations of eastern and western boreal fire histories to compare the site investigated in this study. Sites within the boreal region and with radiocarbon ages (**Fig. 1**; boreal region defined after Levavasseur et al. 2012) were extracted and analyzed using the "paleofire" package in R (Blarquez et al. 2014). The boundary of 82 °W was used to separate western and eastern boreal sites, based on paleoclimate data from sites in western Ontario (Lake 239; **Fig. 1**; Moos and Cumming 2012). Each record was transformed prior to compilation by scaling the records between 0 and 1, Box-Cox normalization, and converting to a z-score with the base period set to the last 8000 years (Power et al. 2010). All sites were lake sediment records, which provide a more regional signal than peat charcoal records, and all had influx data. The composite curve for each region was created using the "pfComposite" function in the "paleofire" package (Blarquez et al. 2014). The composite was the mean z-score in 500 year bins, with bootstrap resampling (1000 iterations). We selected 500 year bins to match the lowest sample resolution in the included studies (# of samples divided by the length of record; see **Tables S1** and **S2**).

3. Results

3.1. Chronology, peat properties, carbon accumulation rates

Peat accumulation initiated at all three coring localities by 5600 cal yr BP or earlier (**Table 1**; **Fig. 2**). All three coring locations are interpreted to have rapidly transitioned to either treed poor fen or bog conditions after initiation, with the presence of significant *Sphagnum* moss and ligneous (woody) plant remains throughout the cores, including the consistent occurrence of conifer needles (**Fig. 3**, Vitt 2006; Loisel et al. 2014). Rapid succession (i.e., from marsh and/or rich fen conditions or from forest to wetland through paludification) can occur in relatively drier localities controlled by local topography and drainage (Klinger and Short 1996; Glaser et al. 2004). Further, paludification can be accelerated by fire, and since there are high charcoal concentrations at the base of two cores, fire at

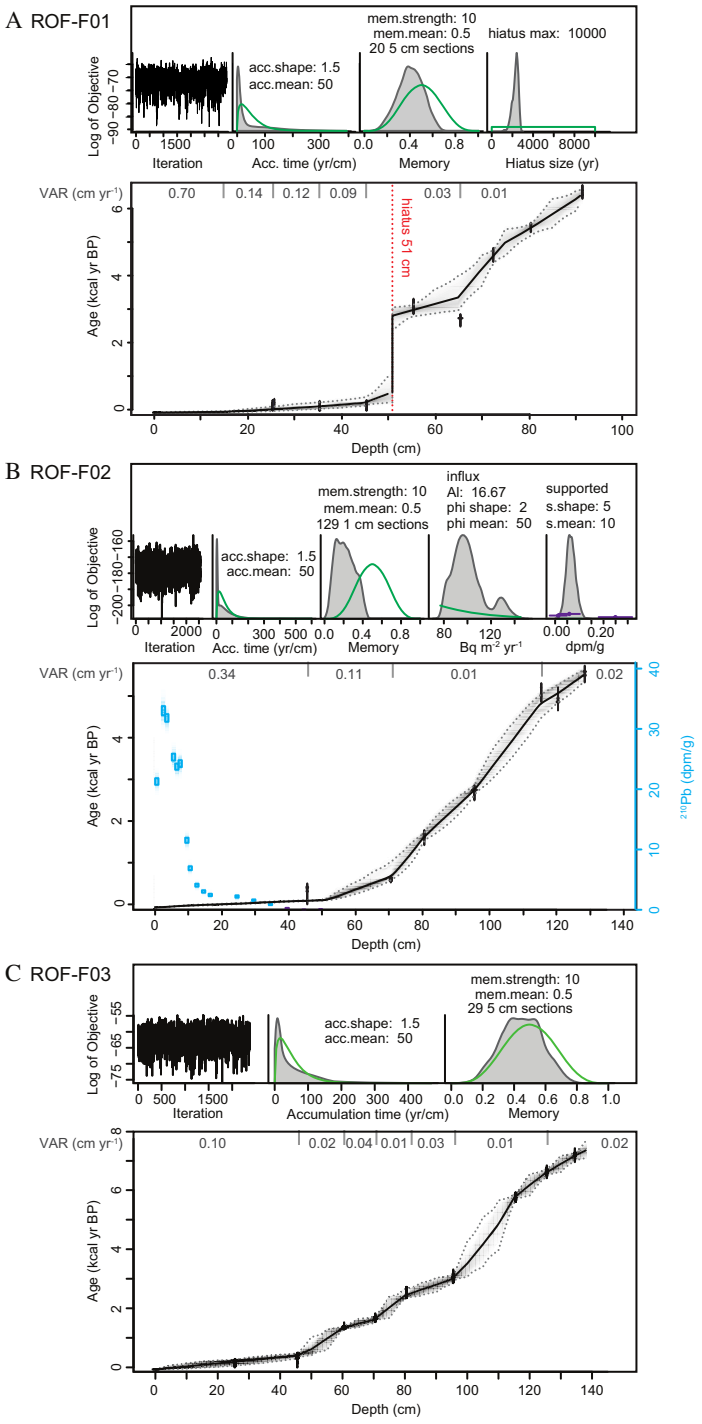

Fig. 2. Bayesian age-depth model outputs for ROF-F01, ROF-F02, and ROF-F03, western Hudson Bay Lowlands, Canada (Blaauw and Christen 2011; Blaauw et al. 2021). Black line is the weighted mean age and the darker the greyscale within the 95% confidence interval, the more likely the age, based on Markov Chain Monte Carlo (MCMC) iterations. Dashed lines are the 95% confidence intervals. ^{210}Pb activities and their error are plotted for ROF-F02 in blue (B). Vertical accretion rates (VARs) labeled above each age-depth plot are the mean for the interval between the corresponding radiocarbon ages. acc. = accumulation; mem. = memory.

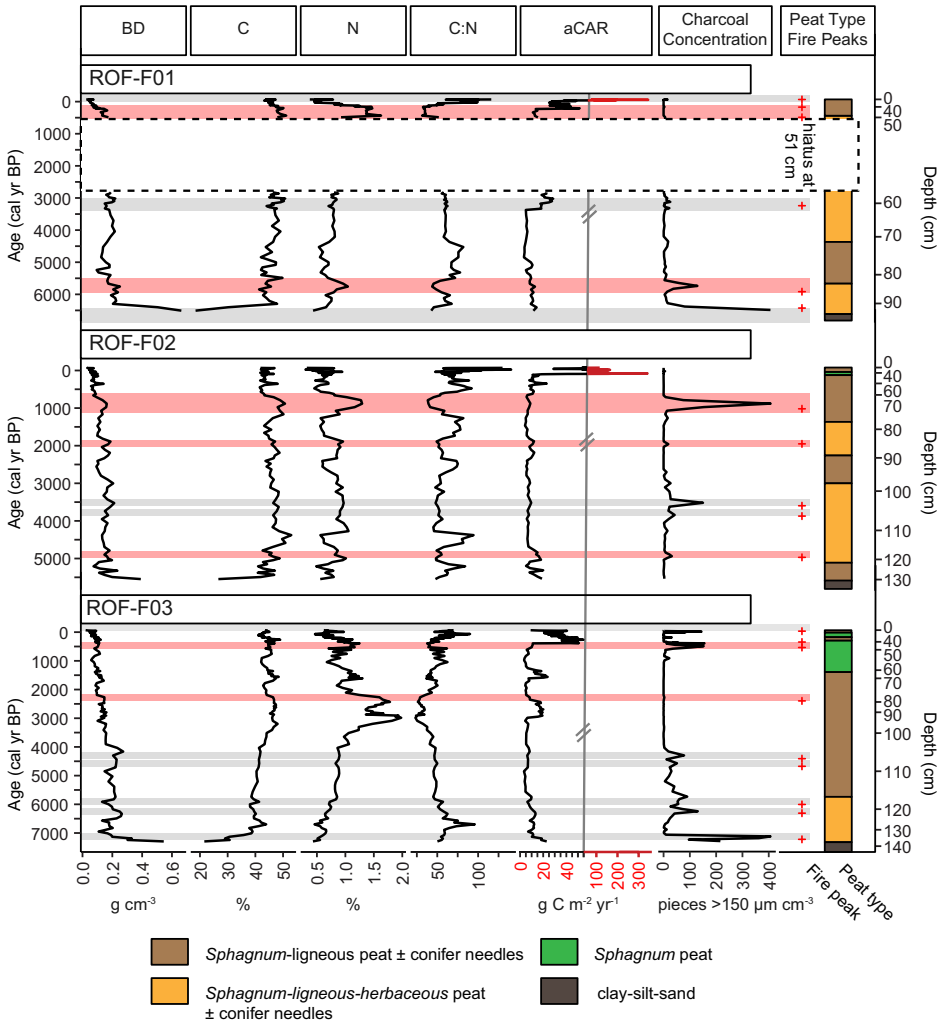

Fig. 3. Peat properties, charcoal concentration, and fire peaks for ROF-F01, ROF-F02, and ROF-F03, western Hudson Bay Lowlands, Canada. Age is the primary axis. BD: bulk density; aCAR: apparent carbon accumulation rate. Fire peaks correspond to peaks identified by CharAnalysis as shown in Fig. 4 with horizontal bars linking fire peaks to C:N ratio values. Fire peaks associated with shifts to C:N ratios lower than the mean for the site are in red and indicate peat smoldering (Zaccone et al. 2014).

the site in this study may have also promoted terrestrial to wetland succession variably across the study region and explain the large spread in basal ages (Simard et al. 2007; Magnan et al. 2018).

At all three coring localities, peat properties (BD and C:N ratio) generally vary with either peat type and (or) charcoal concentration, while aCARs are predominantly related to shifts in vertical accretion rate in the age-depth model (Figs. 2 and 3). Further, shifts in broad peat types do not correspond to changes in charcoal concentrations, suggesting that the Holocene fire records for the study region are reflective of changes in regional climatic conditions and not vegetation change (Fig. 3). At ROF-F01 (edge of burned area), shifts in C:N ratio broadly correspond to shifts in peat type. A hiatus was placed in the record at 51 cm, between the two radiocarbon ages where the deposition time was greater than 400 yr·cm^{-1} (Fig. 2). The highest nitrogen content is above the hiatus in the record, reaching 1.4–1.6 % between 180 and 400 cal yr BP (Fig. 3). High nitrogen content and the corresponding low C:N ratio in relation

to the hiatus indicate peat smoldering (Zaccone et al. 2014) and support the placement of the hiatus. At ROF-F02 (adjacent to burned area), C:N ratios are more variable, along with peat type (Fig. 3). The highest nitrogen values at the coring location correspond to the highest charcoal concentration in the record, also suggesting that N was enriched with peat smoldering (Fig. 3; Zaccone et al. 2014). At ROF-F03 (center of burned area), the lower portion of the record (>4000 cal yr BP) has higher peat bulk density that corresponds to lower C and N content and relatively high charcoal concentration (Fig. 3). Unlike the other two coring locations, herbaceous material as a major component of the peat type is restricted to lower portion of the core (>5800 cal yr BP). Further, *Sphagnum* peat predominates in the uppermost portion (above 65 cm or 1500 cal yr BP). High nitrogen content occurs between 2300 and 3300 cal yr BP, reaching values of up to 1.9% (Fig. 3). A fire peak lies within this interval, but charcoal concentration is low (Fig. 3). All cores have high aCARs associated with high vertical accretion rates in the uppermost acrotelm peat (Figs. 2 and 3).

Differences between LORCA, carbon density, and total carbon mass at the coring locations correspond to differences in basal age and depth, microtopography, and vegetation cover (Table 1). Mean carbon density ranged from 47 to 57 kg C m^{-3} for the three coring localities, with higher carbon densities in the shrub-rich portions of the burned area with older basal ages and that were collected from hummocks (i.e., ROF-F01 and ROF-F03). Total carbon mass of the peat profiles was the highest at the oldest coring locality (ROF-F03) and lowest at the site with the shallowest peat depth (ROF-F01). LORCAs for the sites were between 8 and 11 g C $m^{-2}{\cdot}yr^{-1}$, with the highest occurring in the treed core locality in a hollow (ROF-F02; Table 1).

3.2. Charcoal accumulation rates, fire frequency, and potential carbon loss

The rescaled CHARs (median resolution) range from 0 to 8 pieces $cm^{-2}{\cdot}yr^{-1}$ for all coring locations (Fig. 4). A total of five to nine fire peaks per core were identified. All peaks across the three cores are well separated from C_{noise}, since the median SNI was >3 globally, locally for more than 85% of the samples in each core, and for each significant peak (Table 1; Kelly et al. 2011). One fire peak was also placed at the top of the hiatus of ROF-F01 independent of the peak determination in CharAnalysis, as we interpret this hiatus to be caused by peat combustion. The upper boundary of the hiatus also corresponds to fire peaks in the two other records when accounting for age error (i.e., within the 95% CI; Fig. 4). At each coring locality, 3–4 peaks were associated with a shift in C:N ratio that was lower than the core mean, suggesting peat smoldering occurred (Table 1 and Fig. 3). Further, increased CHARs are recorded in the uppermost portion of the record at every coring locality, but fire peaks are only significant for the cores within the burned area (i.e., ROF-F01 and ROF-F03; Figs. 1 and 4). Only the age of the uppermost significant peak at ROF-F03 matches the year burned (1991). However, the cores within the burned area do not have Pb-210 ages to constrain very recent vertical accretion rates, as we did not perform Pb-210 dating where disturbance from the most recent fire occurred (Fig. 2). The age range surrounding the increased CHARs that were not significant at the unburned coring locality (ROF-F02) also contains the year burned (1991) and is constrained by Pb-210 ages (Fig. 4). Holocene-scale FRIs (0–8000 cal yr BP) and their corresponding fire frequencies were similar for the three cores, ranging from 907 to 990 years and 1.0 to 1.1 fires $1000{\cdot}yr^{-1}$, respectively (Table 1). As a result of fire at the site, we estimate that 8–12 kg C m^{-2} was lost to the atmosphere over the site's accumulation history (Table 1).

The fire records at the coring localities generally record similar timing in fire peaks, with at least 70% of the fire peaks overlapping in age with at least one other peak (Fig. 4). However, some peaks are independent despite the localities being < 100 m apart from each other, even when age error is considered (Figs. 1 and 4). Local-scale variability in charcoal records has been demonstrated on

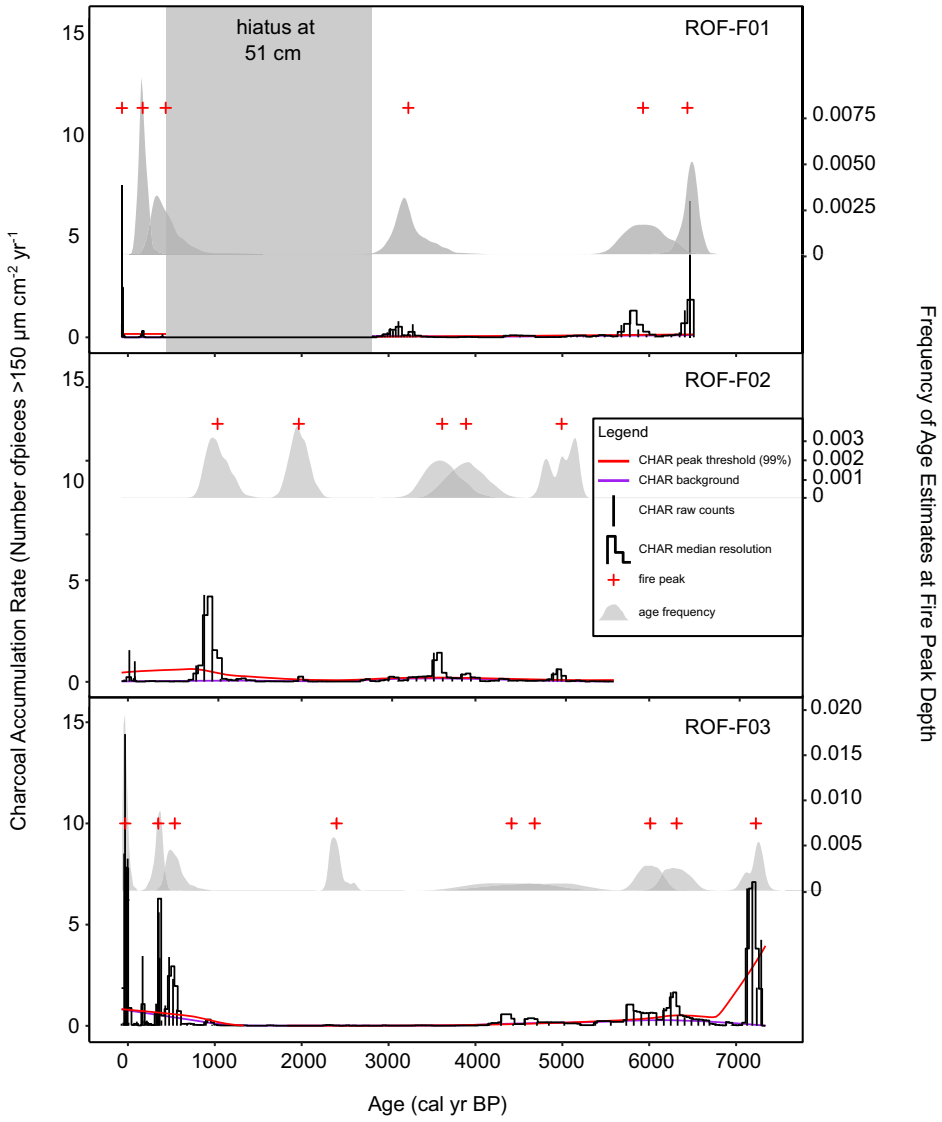

Fig. 4. Charcoal accumulation rates (CHAR) and age error estimates for identified fire peaks for ROF-F01, ROF-F02, and ROF-F03, western Hudson Bay Lowlands margin, Canada.

replicate and site-level records in other peatlands, as well as at various charcoal size fractions, suggesting that peatland charcoal records are highly localized to the core location (e.g., van Bellen et al. 2012; Cui et al. 2020; Beaulne et al. 2021). However, the FRIs through the Holocene for each of the core localities fit within the upper end of modern estimates of FRIs for the HBL (200–1000 years; Stocks et al. 2002; Boulanger et al. 2014; Coops et al. 2018). Therefore, the paleo-fire return intervals recorded at the site match regional expectations.

Overall, more fires occurred in the Middle Holocene in comparison to the Late Holocene. When individual FRIs from across the three coring locations were pooled to investigate Middle (4200–7200 cal yr BP) and Late Holocene (500–4200 cal yr BP) differences, the median FRI for the Middle Holocene (912 years) was lower than the Late Holocene (1650 years), corresponding to a

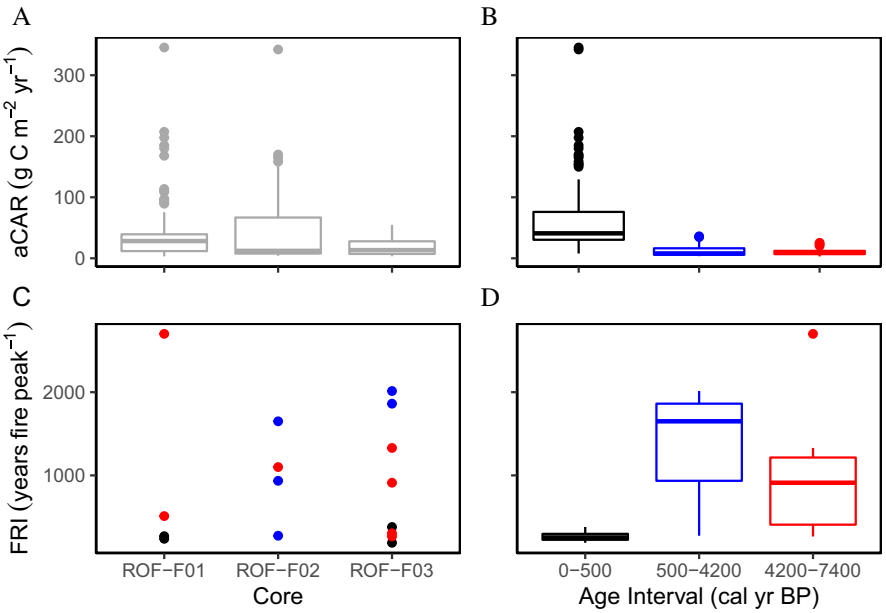

Fig. 5. Boxplots and individual data points of apparent carbon accumulation rates (aCARs) and fire return intervals (FRIs) for ROF-F01, ROF-F02, and ROF-F03, organized by site (A,C) and age interval (B,D). aCARs in A include acrotelm rates (0–500 cal yr BP). The black, blue, and red dots in C correspond to the time bins in B and D, and correspond to the 0–500 cal yr BP, 500–4200 cal yr BP, and 4200–7200 cal yr BP, respectively. Each point in C is the time between individual charcoal peaks in each core through time.

higher median fire frequency (1.1 vs. 0.6 fires 1000·yr^{-1}; Figs. 5 and 6) and subsequent carbon loss (6 kg C m^{-2} vs. 3 kg C m^{-2}) across the interval. Fire frequency patterns at the site match the trend in the western boreal compilation, where there were higher CHARs within lake records during the Middle Holocene, signaling more fire on the landscape during that time (Fig. 6).

3.3. Relationship between fire frequency and carbon accumulation rates

The relationship between changing fire frequencies and peatland carbon accumulation differed when investigating at a local vs. regional scale. aCARs were not significantly different between the Middle and Late Holocene at the study site in the combined core dataset ($W = 4352$, $p = 0.609$; Fig. 5), despite differing median fire frequency between the time bins. However, when LORCA and fire frequency from this study are plotted with other boreal sites that represent a larger dataset across a larger fire frequency and moisture gradient, there is a significant relationship, with decreasing Holocene-scale carbon accumulation rates with increasing fire frequency (Fig. 7).

4. Discussion

4.1. Relationships between fire frequency and Holocene climate

Median fire frequency recorded from the study region is related to differing hydroclimatic conditions between the Middle and Late Holocene. Higher median fire frequency in the Middle Holocene corresponds to warmer conditions with minimal precipitation change in the HBL (<0.5 °C; Fig. 6; pollen-inferred estimates; Hargan et al. 2020), which has been linked to relatively drier conditions in testate amoeba records because of higher evaporative demand (Fig. 6; Davies et al. 2021). Further, the

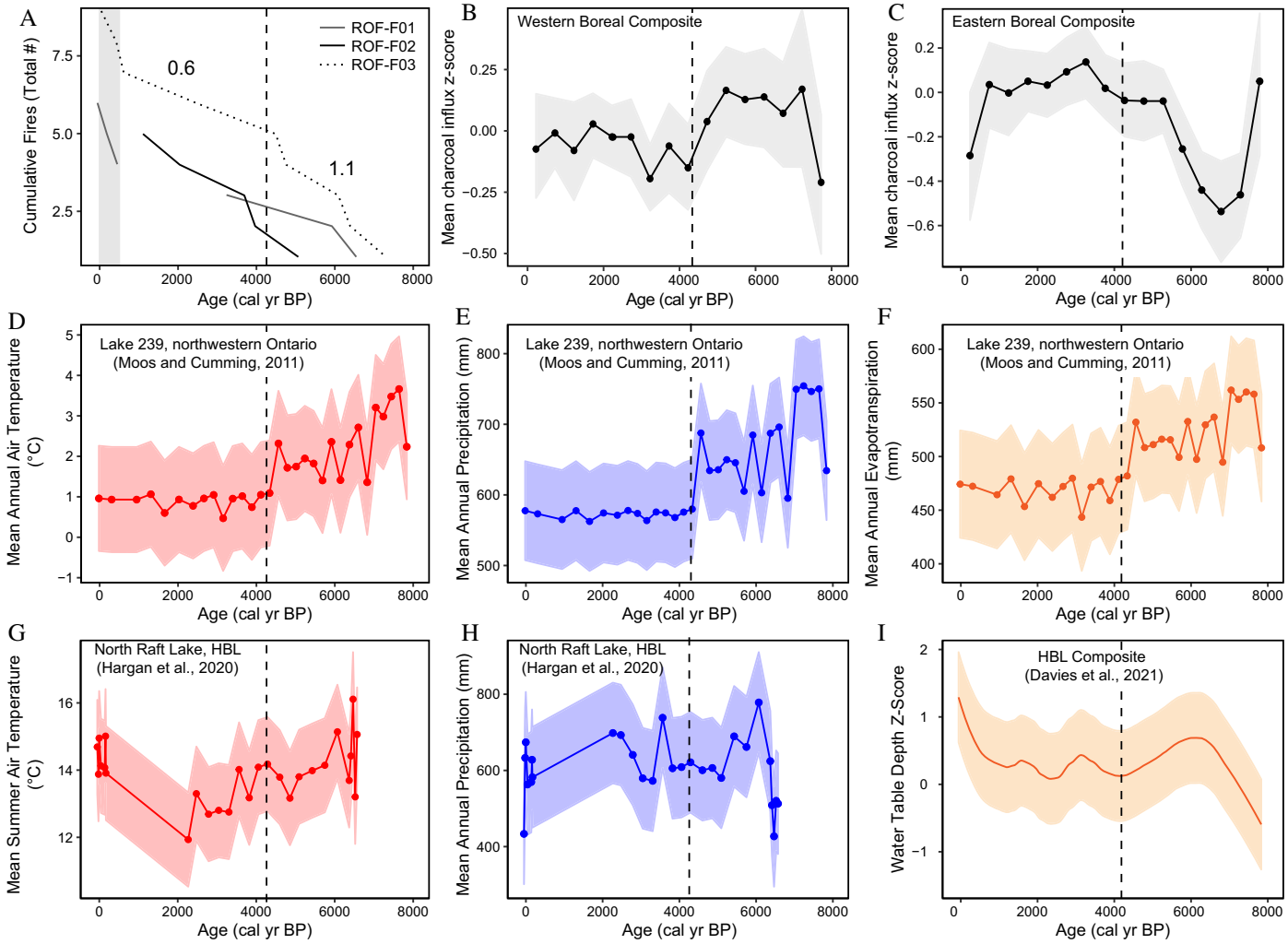

Fig. 6. Comparison of fire frequency from ROF-F01, ROF-F02, and ROF-F03 to other regional paleoecological records. (A) Cumulative fires for ROF-F01, ROF-F02, and ROF-F03. Labeled slope for each interval is the median fire frequency from the combined core data in fires 1000·yr^{-1}. Grey shaded area is the last 500 years, which were excluded from the Late Holocene fire frequency calculation. (B) Mean z-score of normalized charcoal influx data from the western boreal region (500 year bins; Global Charcoal Database; see **Fig. 1** and **Table S1**). Higher z-score values correspond to higher relative influx of charcoal into lake records. (C) Mean z-score of normalized charcoal influx data from the eastern boreal region (500 year bins; Global Charcoal Database; see **Fig. 1** and **Table S2**). Higher z-score values correspond to higher relative influx of charcoal into lake records. (D–F) Annual temperature, precipitation, and evapotranspiration reconstructions from a pollen record from Lake 239, northwestern Ontario (Moos and Cumming 2011). (G–H) Summer temperature and annual precipitation reconstructions from a pollen record from North Raft Lake, Hudson Bay Lowlands (HBL; Hargan et al. 2020). (I) Locally weighted least squares regression of normalized testate amoeba water table depth reconstructions from the HBL region (Davies et al. 2021). Higher z-score values correspond to drier relative conditions.

pattern at the study site is also comparable to Lake 239 record in northwestern Ontario, where despite higher precipitation within the Middle Holocene, higher evaporative demand and likely more instances of prolonged summer drought led to higher fire frequency surrounding the site (12.5 fires 1000·yr^{-1} in the Middle Holocene and <5 fires 1000 yr^{-1} in the Late Holocene; Moos and Cumming 2011; 2012; **Fig. 6**). Because a difference in median fire frequency is recorded between these time periods at the study region, fire frequency is apparently impacted by relatively small

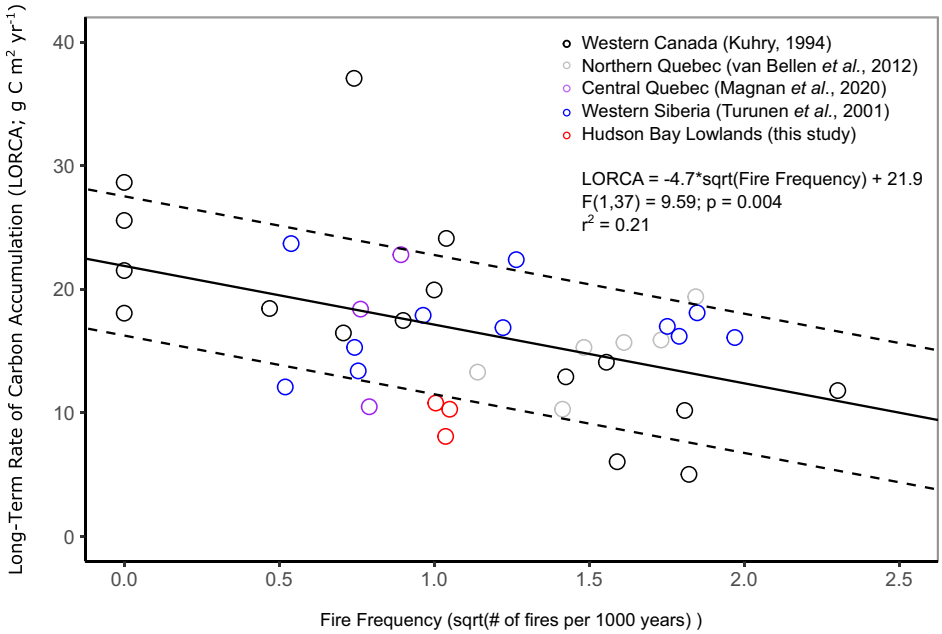

Fig. 7. Relationship between peatland fire frequency and Holocene-scale carbon accumulation rate (LORCA) from North American and Siberian boreal sites. Dashed line is the residual standard error of the linear regression model (± 5.6 g C m^{-2}·yr^{-1}).

changes in temperature and evapotranspiration budgets and therefore supports that some HBL peatlands may be increasingly vulnerable to fire because of anthropogenic climate change.

Different fire frequency patterns between the site and the eastern boreal compilation support that regional factors are causing alternate fire regimes. In the Quebec region, the Middle Holocene was characterized by higher relative humidity associated with less frequent intrusion of cool and dry Pacific air masses (Edwards et al. 1996). Less frequent intrusions meant there were fewer periods of summer drought that could promote fire (Carcaillet and Richard 2000). Since the western HBL has a higher median fire frequency in the Middle Holocene, cool and dry Pacific air masses likely still influenced drought in the region during this time and support that continental air mass movement changes and drought frequency are critical to constrain to predict peatland fire frequency in the future (e.g., Marcisz et al. 2017). However, fire frequency is still comparatively much lower than modern and Holocene fire values for peatlands in western Canadian boreal region, attesting to the site's location at the transition from a continental to more humid climate (i.e., western boreal fire frequency in peatlands is 2–8 fires 1000·yr^{-1}; Kuhry 1994; Zoltai et al. 1998; Wieder et al. 2009).

FRIs shorten over the last 500 years and are smaller than both the Middle and Late Holocene intervals (**Figs. 6** and 7), which we attribute to recent drying as well as decomposition and acrotelm processes. Some northern peatlands have been drying over the last two centuries with climatic and land use changes and are expected to dry out further with anthropogenic climate change and therefore promote increased fire frequency (Turetsky et al. 2015; Swindles et al. 2019). Although these factors may in part explain the trends in fire frequency at the site, the median fire frequency recorded from the pooled dataset in the last 500 years (3.3 fires 1000·yr^{-1}) is over three times higher than the warmer Middle Holocene value, suggesting that factors other than climate are needed to explain large differences. Decomposition can cause the broadening of charcoal peaks and may disguise smaller

peaks as a result (Camill et al. 2009). Further, fire severity may impact whether charcoal layers are formed or not in the peat column (Turetsky et al. 2004). Therefore, our Middle Holocene estimate could be a conservative estimate of fire frequency in this interval. Charcoal fragments could also potentially move in the acrotelm, which may cause artificial peaks and increase the apparent number of fires (Turetsky et al. 2004). However, we aimed to minimize this through determining background charcoal in CharAnalysis (van Bellen et al. 2012). Overall, due to these processes, the acrotelm and catotelm fire frequencies are challenging to compare.

4.2. Fire frequency impacts on peatland carbon cycling

aCARs at the site were not significantly different between the Middle and Late Holocene and do not correspond to changes in median fire frequency, suggesting that carbon losses may have been offset by other local factors (**Fig. 5**). The Middle Holocene has also been linked to higher biomass production with longer growing degree days above zero in northern peatlands (Yu et al. 2010). Higher vegetation inputs into the site between fires may have therefore compensated for some of the loss. *Sphagnum* macrofossils are also consistently found throughout each core, suggesting rapid recovery from fire (**Fig. 3**, Magnan et al. 2012). Further, charcoal peaks are not always associated with evidence of peat smoldering (**Fig. 3** and **Table 1**). Therefore, *Sphagnum* moss was able to protect the deeper soils by preventing water loss in most cases (Benscoter and Wieder 2003; Benscoter et al. 2011). Fire may have also offset carbon losses at the site by stabilizing a fraction of the organic matter through charcoal production (Heinemeyer et al. 2018; Flanagan et al. 2020; Pellegrini et al. 2021). Chemical alteration of peat at the site during fire is supported by the low C:N ratios and high nitrogen content that are linked to some of the charcoal peaks in the cores (Zaccone et al. 2014). Therefore, the records in this study demonstrate the complex interactions between fire and carbon storage that are dependent on local factors, including whether fire directly or indirectly impacts the peat column.

Fire frequency and carbon accumulation relationships vary at local scales. This variation implies that while fire can play a role in removing carbon inputs, regional compilations are clearly needed to predict the relative role of fire on the global peatland carbon balance. Within local studies in boreal peatlands, both positive and negative relationships between fire frequency and LORCAs have been demonstrated (Kuhry 1994; Camill et al. 2009; van Bellen et al. 2012; Magnan et al. 2020) and, depending on the region, local factors including hydrological conditions (van Bellen et al. 2012), vegetation composition (Camill et al. 2009), and decomposition prevention (Heinemeyer et al. 2018) compensated for any impacts on carbon accumulation rates. When sites are pooled from boreal regions that represent a larger gradient in fire frequency and moisture balance conditions seen across the Holocene than at an individual site, we demonstrate that there is a significant negative relationship between fire frequency and LORCA, with considerable variation (**Fig. 7**). The variation supports that some peatlands will be more resilient to carbon loss from fire than others (Ingram et al. 2019). Resilience has been shown to come from vegetation composition (i.e., *Sphagnum* moss abundance and recovery; Magnan et al. 2012; Kettridge et al. 2015) and hydrogeological setting (Hokanson et al. 2016; Ingram et al. 2019). At our study site, LORCA values are lower than predicted based on the sites fire frequency in the linear regression model (**Fig. 7**). Further, the estimated total carbon loss from each coring locality does not fully explain lower LORCAs at the site from median HBL values (18.3 g C $m^{-2}{\cdot}yr^{-1}$; Packalen and Finkelstein 2014; **Table 1**). Therefore, the dry conditions at the site needed for higher tree cover also likely contributed further to lowering carbon stocks (Magnan et al. 2020; Beaulne et al. 2021). Therefore, as expected, sites with dry conditions and high tree and shrub cover are more vulnerable to fire and will likely have an even more diminished long-term carbon storage if more frequent fire occurs.

Although only subtle changes in median fire frequency were recorded at the site with modest mean summer temperature changes within the Middle Holocene (**Fig. 6**; Hargan et al. 2020), these changes

also have implications for carbon release across the Holocene. When comparing the median Middle and Late Holocene FRI of the study site, emissions were potentially doubled per unit area between the Middle and Late Holocene, despite minimal annual temperature increases (Hargan et al. 2020). Therefore, characterizing the FRI in HBL peatlands has the potential to constrain the atmospheric inputs from fire on a regional and global scale through the Holocene. However, continued work capturing spatial variability in peatland fire frequency changes across the region is needed to support scaling fluxes from fire (Loisel et al. 2017).

5. Conclusions

Median fire frequency for our study site on the western HBL margin was higher in the Middle Holocene despite only modest (<0.5 °C) changes in mean summer temperatures (Hargan et al. 2020). Subsequently, the potential carbon released during the Middle Holocene was potentially 50% higher than in the Late Holocene at the site. The record matches western Canadian boreal fire frequency pattern and indicates that length of summer drought is an important distinction between western and eastern boreal zones in North America. A lower overall fire frequency across the Holocene at the site compared to western Canadian boreal sites, however, supports that the HBL region lies between the continental and humid climate regimes (Zoltai et al. 1998). We demonstrate that local factors can diminish impacts of fire on shifting aCARs, but when sites across the boreal region globally are combined and a larger moisture and fire frequency gradient is investigated, fire frequency can explain some of the variation in LORCAs over the Holocene. Therefore, with future warming, some peatlands of the HBL may be more vulnerable to fire and, as a result, may weaken their ability to be net carbon sinks.

Acknowledgements

We thank A. Brunet, M. Mack, J. Moonias, and S. Reed for field assistance; A. Copeland for laboratory assistance; G. Labrecque for carbon and nitrogen analysis; C. Grondahl for field preparation assistance; B. Cumming and D. Danesh for providing the reconstruction data from Lake 239; and A. Loder for assistance with charcoal imagery. The data used to create the charcoal compilation curves in **Fig. 6** were obtained from the Global Charcoal Database (paleofire.org); we thank the data contributors and the Global Palaeofire Working Group for their work. A list of the original publications for the charcoal records is found in **Tables S1** and **S2**. Funding for this project was from Natural Sciences and Engineering Research Council of Canada (NSERC) grants to S. Finkelstein, a NSERC-Post Graduate Scholarship and Canadian Quaternary Association (CANQUA) Alexis Dreimanis Award to M. Davies, and the Government of Ontario.

Author contributions

MAD, JWM, MSP, and SAF conceived and designed the study. MAD performed the experiments/collected the data. MAD analyzed and interpreted the data. JWM, MSP, and SAF contributed resources. MAD, JWM, MSP, and SAF drafted or revised the manuscript.

Competing interests

The authors have declared that no competing interests exist.

Data availability

Raw charcoal counts, carbon and nitrogen content, and bulk density data will be made available within the Global Charcoal Database and Neotoma upon publication. (paleofire.org and neotomadb.org/).

Supplementary material

The following Supplementary Material is available with the article through the journal website at doi:10.1139/facets-2022-0162.

Supplementary Material 1

References

Balshi MS, McGuire AD, Duffy P, Flannigan M, Kicklighter DW, and Melillo J. 2009. Vulnerability of carbon storage in North American boreal forests to wildfires during the 21st century. Global Change Biology, 15(6): 1491–1510. DOI: 10.1111/j.1365-2486.2009.01877.x

Barnett PJ, Yeung KH, and McCallum JD. 2013a. Surfical Geology of the Lansdowne House Area Southeast, Northern Ontario (Map P3710): Ontario Ministry of Energy. Northern Development, and Mines, scale 1: 100000.

Barnett PJ, Yeung KH, and McCallum JD. 2013b. Surficial Geology of the Lansdowne House Area Northeast, Northern Ontario (Map P3697): Ontario Ministry of Energy. Northern Development and Mines, scale 1: 100000.

Beaulne J, Garneau M, Magnan G, and Boucher É. 2021. Peat deposits store more carbon than trees in forested peatlands of the boreal biome. Scientific Reports, 11(1): 2657. PMID: 33514778 DOI: 10.1038/s41598-021-82004-x

Benscoter BW, Thompson DK, Waddington JM, Flannigan MD, Wotton BM, de Groot WJ, et al. 2011. Interactive effects of vegetation, soil moisture and bulk density on depth of burning of thick organic soils. International Journal of Wildland Fire, 20(3): 418–429. DOI: 10.1071/WF08183

Benscoter BW, and Wieder RK. 2003. Variability in organic matter lost by combustion in a boreal bog during the 2001 Chisholm fire. Canadian Journal of Forest Research, 33(12): 2509–2513. DOI: 10.1139/x03-162

Blaauw M, Andres Christen J, and Aquino-Lopez MA. 2021. rplum: Bayesian age-depth modelling of 210Pb-dated cores, R package version 0.2.1.

Blaauw M, and Christen JA. 2011. Flexible paleoclimate age-depth models using an autoregressive gamma process. Bayesian Analysis, 6(3): 457–474. DOI: 10.1214/ba/1339616472

Blarquez O, Vannière B, Marlon JR, Daniau A-L, Power MJ, Brewer S, and Bartlein PJ. 2014. Paleofire: An R package to analyse sedimentary charcoal records from the Global Charcoal Database to reconstruct past biomass burning. Computers and Geosciences, 72: 255–261. DOI: 10.1016/j.cageo.2014.07.020

Boulanger Y, Gauthier S, and Burton PJ. 2014. A refinement of models projecting future Canadian fire regimes using homogeneous fire regime zones. Canadian Journal of Forest Research, 44(4): 365–376. DOI: 10.1139/cjfr-2013-0372

Brandt JP. 2009. The extent of the North American boreal zone. Environmental Reviews, 17: 101–161. DOI: 10.1139/A09-004

Bronk Ramsey C. 2009. Bayesian analysis of radiocarbon dates. Radiocarbon, 51(1): 337–360. DOI: 10.1017/S0033822200033865

Camill P, Barry A, Williams E, Andreassi C, Limmer J, and Solick D. 2009. Climate-vegetation-fire interactions and their impact on long-term carbon dynamics in a boreal peatland landscape in northern Manitoba, Canada. Journal of Geophysical Research. Biogeosciences, 114: G04017. DOI: 10.1029/2009JG001071

Canadian Forest Service. 2020, National Burned Area Composite (NBAC), Natural Resources Canada. [online]: Available from cwfis.cfs.nrcan.gc.ca.

Carcaillet C, and Richard PJH. 2000. Holocene changes in seasonal precipitation highlighted by fire incidence in eastern Canada: Climate Dynamics, 16(7): 549–559. DOI: 10.1007/s003820000062

Chambers FM, Beilman DW, and Yu Z. 2010. Methods for determining peat humification and for quantifying peat bulk density, organic matter and carbon content for palaeostudies of climate and peatland carbon dynamics. Mires and Peat, 7, Article 7, 1–10.

Chaudhary N, Westermann S, Lamba S, Shurpali N, Sannel ABK, Schurgers G., et al. 2020. Modelling past and future peatland carbon dynamics across the pan-Arctic. Global Change Biology, 26(7): 4119–4133. PMID: 32239563 DOI: 10.1111/gcb.15099

Coops NC, Hermosilla T, Wulder MA, White JC, and Bolton DK. 2018. A thirty year, fine-scale, characterization of area burned in Canadian forests shows evidence of regionally increasing trends in the last decade. PLoS ONE, 13(5): e0197218. PMID: 29787562 DOI: 10.1371/journal.pone.0197218

Cui Q-Y, Gaillard M-J, Vannière B, Colombaroli D, Lemdahl G, Olsson F, et al. 2020. Evaluating fossil charcoal representation in small peat bogs: Detailed Holocene fire records from southern Sweden: The Holocene, 30(11): 1540–1551. DOI: 10.1177/0959683620941069

Davies MA, McLaughlin JW, Packalen MS, and Finkelstein SA. 2021. Using Water Table Depths Inferred From Testate Amoebae to Estimate Holocene Methane Emissions From the Hudson Bay Lowlands, Canada. Journal of Geophysical Research: Biogeosciences, 126(2): e2020JG005969. DOI: 10.1029/2020JG005969

Ecological Stratification Working Group. 1995. Terrestrial Ecozones and Ecoregions of Canada. Agriculture and Agri-Food and Environment Canada, scale, 1: 7500000.

Edwards TWD, Wolfe BB, and MacDonald GM. 1996. Influence of changing atmospheric circulation on precipitation δ18O-temperature relations in Canada during the Holocene. Quaternary Research, 46(3): 211–218. DOI: 10.1006/qres.1996.0061

Erni S, Wang X, Taylor S, Boulanger Y, Swystun T, Flannigan M, et al. 2019. Developing a two-level fire regime zonation system for Canada. Canadian Journal of Forest Research, 50(3): 259–273. DOI: 10.1139/cjfr-2019-0191

Flanagan NE, Wang H, Winton S, and Richardson CJ. 2020. Low-severity fire as a mechanism of organic matter protection in global peatlands. Thermal alteration slows decomposition. Global Change Biology, 26(7): 3930–3946. PMID: 32388914 DOI: 10.1111/gcb.15102

Flannigan M, Stocks B, Turetsky M, and Wotton M. 2009. Impacts of climate change on fire activity and fire management in the circumboreal forest: Global Change Biology, 15(3): 549–560. DOI: 10.1111/j.1365-2486.2008.01660.x

Gallego-Sala AV, Charman DJ, Brewer S, Page SE, Prentice IC, Friedlingstein P, et al. 2018. Latitudinal limits to the predicted increase of the peatland carbon sink with warming. Nature Climate Change, 8(10): 907–913. DOI: 10.1038/s41558-018-0271-1

Gavin DG, Hu FS, Lertzman K, and Corbett P. 2006. Weak climatic control of stand-scale fire history during the Late Holocene. Ecology, 87(7): 1722–1732. PMID: 16922322 DOI: 10.1890/0012-9658(2006)87[1722:WCCOSF]2.0.CO;2

Glaser PH, Hansen BCS, Siegel DI, Reeve AS, and Morin PJ. 2004. Rates, pathways and drivers for peatland development in the Hudson Bay Lowlands, northern Ontario, Canada: Journal of Ecology, 92(6): 1036–1053. DOI: 10.1111/j.0022-0477.2004.00931.x

Gorham E. 1991. Northern peatlands - role in the carbon-cycle and probable responses to climatic warming: Ecological Applications, 1(2): 182–195. PMID: 27755660 DOI: 10.2307/1941811

Government of Canada. 2021. Canadian Climate Normals 1971-2000 Station Data [online]: Available from climate.weather.gc.ca/climate_normals/index_e.html,

Government of Ontario. 2021. Far North Land Cover, scale 1:100,000.

Hall RJ, Skakun RS, Metsaranta JM, Landry R, Fraser RH, Raymond DA, et al. 2020. Generating annual estimates of forest fire disturbance in Canada: The National Burned Area Composite: International Journal of Wildland Fire, 29: 878–891. DOI: 10.1071/WF19201

Hargan KE, Finkelstein SA, Rühland KM, Packalen MS, Dalton AS, Paterson AM, et al. 2020. Post-glacial lake development and paleoclimate in the central Hudson Bay Lowlands inferred from sediment records. Journal of Paleolimnology, 64(1): 25–46. DOI: 10.1007/s10933-020-00119-z

Heinemeyer A, Asena Q, Burn WL, and Jones AL. 2018. Peatland carbon stocks and burn history: Blanket bog peat core evidence highlights charcoal impacts on peat physical properties and long-term carbon storage: Geo: Geography and Environment, 5(2): e00063. DOI: 10.1002/geo2.63

Helbig M, Waddington JM, Alekseychik P, Amiro BD, Aurela M, Barr AG, et al. 2020. Increasing contribution of peatlands to boreal evapotranspiration in a warming climate. Nature Climate Change, 10(6): 555–560. DOI: 10.1038/s41558-020-0763-7

Higuera P. 2009. CharAnalysis 0.9: Diagnostic and analytical tools for sediment-charcoal analysis.

Higuera PE, Brubaker LB, Anderson PM, Hu FS, and Brown TA. 2009. Vegetation mediated the impacts of postglacial climate change on fire regimes in the south-central Brooks Range, Alaska. Ecological Monographs, 79(2): 201–219. DOI: 10.1890/07-2019.1

Higuera PE, Gavin DG, Bartlein PJ, and Hallett DJ. 2010. Peak detection in sediment–charcoal records: Impacts of alternative data analysis methods on fire-history interpretations. International Journal of Wildland Fire, 19(8): 996–1014. DOI: 10.1071/WF09134

Hokanson KJ, Lukenbach MC, Devito KJ, Kettridge N, Petrone RM, and Waddington JM. 2016. Groundwater connectivity controls peat burn severity in the boreal plains: Ecohydrology, 9(4): 574–584. DOI: 10.1002/eco.1657

Ingram RC, Moore PA, Wilkinson S, Petrone RM, and Waddington JM. 2019. Postfire soil carbon accumulation does not recover boreal peatland combustion loss in some hydrogeological settings. Journal of Geophysical Research: Biogeosciences, 124(4): 775–788. DOI: 10.1029/2018JG004716

Kasischke ES, and Bruhwiler LP. 2002. Emissions of carbon dioxide, carbon monoxide, and methane from boreal forest fires in 1998. Journal of Geophysical Research: Atmospheres, 108(D1): FFR 2-14. DOI: 10.1029/2001JD000461

Kasischke ES, and Turetsky MR. 2006. Recent changes in the fire regime across the North American boreal region—Spatial and temporal patterns of burning across Canada and Alaska. Geophysical Research Letters, 33(9). DOI: 10.1029/2006GL025677

Kelly RF, Higuera PE, Barrett CM, and Hu FS. 2011. A signal-to-noise index to quantify the potential for peak detection in sediment–charcoal records. Quaternary Research, 75(1): 11–17. DOI: 10.1016/j.yqres.2010.07.011

Kettridge N, Turetsky MR, Sherwood JH, Thompson DK, Miller CA, Benscoter BW, et al. 2015. Moderate drop in water table increases peatland vulnerability to post-fire regime shift. Scientific Reports, 5(1): 8063. DOI: 10.1038/srep08063

Klinger LF, and Short SK. 1996. Succession in the Hudson Bay Lowland, northern Ontario, Canada. Arctic and Alpine Research, 28(2): 172–183. DOI: 10.2307/1551757

Kuhry P. 1994. The role of fire in the development of *Sphagnum*-dominated peatlands in western boreal Canada. Journal of Ecology, 82(4): 899–910. DOI: 10.2307/2261453

Levavasseur G, Vrac M, Roche DM, and Paillard D. 2012. Statistical modelling of a new global potential vegetation distribution. Environmental Research Letters, 7(4): 044019. DOI: 10.1088/1748-9326/7/4/044019

Loisel J, Gallego-Sala AV, Amesbury MJ, Magnan G, Anshari G, Beilman DW, et al. 2021. Expert assessment of future vulnerability of the global peatland carbon sink. Nature Climate Change, 11(1): 70–77. DOI: 10.1038/s41558-020-00944-0

Loisel J, van Bellen S, Pelletier L, Talbot J, Hugelius G, Karran D, et al. 2017, Insights and issues with estimating northern peatland carbon stocks and fluxes since the Last Glacial Maximum. Earth Science Reviews, 165: 59–80. DOI: 10.1016/j.earscirev.2016.12.001

Loisel J, Yu ZC, Beilman DW, Camill P, Alm J, Amesbury MJ, et al. 2014. A database and synthesis of northern peatland soil properties and Holocene carbon and nitrogen accumulation. Holocene, 24(9): 1028–1042. DOI: 10.1177/0959683614538073

Lukenbach MC, Devito KJ, Kettridge N, Petrone RM, and Waddington JM. 2015a. Hydrogeological controls on post-fire moss recovery in peatlands. Journal of Hydrology, 530: 405–418. DOI: 10.1016/j.jhydrol.2015.09.075

Lukenbach MC, Hokanson KJ, Moore PA, Devito KJ, Kettridge N, Thompson DK, et al. 2015b. Hydrological controls on deep burning in a northern forested peatland. Hydrological Processes, 29(18): 4114–4124. DOI: 10.1002/hyp.10440

Magnan G, Garneau M, Le Stum-Boivin É, Grondin P, and Bergeron Y. 2020. Long-Term Carbon Sequestration in Boreal Forested Peatlands in Eastern Canada. Ecosystems, 23(7): 1481–1493. DOI: 10.1007/s10021-020-00483-x

Magnan G, Lavoie M, and Payette S. 2012. Impact of fire on long-term vegetation dynamics of ombrotrophic peatlands in northwestern Québec, Canada. Quaternary Research, 77(1): 110–121. DOI: 10.1016/j.yqres.2011.10.006

Magnan G, Le Stum-Boivin É, Garneau M, Grondin P, Fenton N, and Bergeron Y. 2018. Holocene vegetation dynamics and hydrological variability in forested peatlands of the Clay Belt, eastern Canada, reconstructed using a paleoecological approach. Boreas, 48(1): 131–146. DOI: 10.1111/bor.12345

Marcisz K, Galka M, Pietrala P, Miotk-Szpiganowicz G, Obremska M, Tobolski K, et al. 2017. Fire activity and hydrological dynamics in the past 5700 years reconstructed from *Sphagnum* peatlands along the oceanic-continental climatic gradient in northern Poland. Quaternary Science Reviews, 177: 145–157. DOI: 10.1016/j.quascirev.2017.10.018

Martini IP. 2006. The cold-climate peatlands of the Hudson Bay Lowland, Canada: Brief overview of recent work. *In* Peatlands: Evolution and Records of Environmental and Climate Changes. *Edited by* IP Martini, A Martínez Cortizas, and W Chesworth. Elsevier B. V. Amsterdam, The Netherlands. p. 53–83.

McLaughlin JW, and Packalen MS. 2021. Peat Carbon Vulnerability to Projected Climate Warming in the Hudson Bay Lowlands, Canada: A Decision Support Tool for Land Use Planning in Peatland Dominated Landscapes. Frontiers in Earth Science, 9. DOI: 10.3389/feart.2021.650662

Mooney SD, and Tinner W. 2010. The analysis of charcoal in peat and organic sediments. Mires and Peat, 7, Article 9, 1–18.

Moore TR, and Robinson SD. 2000. The influence of permafrost and fire upon carbon accumulation in high boreal peatlands, Northwest Territories, Canada. Arctic, Antarctic, and Alpine Research, 32(2): 155–166. DOI: 10.1080/15230430.2000.12003351

Moos MT, and Cumming BF. 2011. Changes in the parkland-boreal forest boundary in northwestern Ontario over the Holocene. Quaternary Science Reviews, 30(9–10): 1232–1242. DOI: 10.1016/j.quascirev.2011.02.013

Moos MT, and Cumming BF. 2012. Climate–fire interactions during the Holocene: A test of the utility of charcoal morphotypes in a sediment core from the boreal region of north-western Ontario (Canada). International Journal of Wildland Fire, 21(6): 640–652. DOI: 10.1071/WF10117

Müller J, and Joos F. 2021. Committed and projected future changes in global peatlands – continued transient model simulations since the Last Glacial Maximum. Biogeosciences, 18(12): 3657–3687. DOI: 10.5194/bg-18-3657-2021

New SL, Belcher CM, Hudspith VA, and Gallego-Sala AV. 2016, Holocene fire history: Can evidence of peat burning be found in the palaeo-archive?. Mires and Peat, 18, Article 26, 1–11. DOI: 10.19189/MaP.2016.OMB.219

Nichols J, and Peteet D. 2019. Rapid expansion of northern peatlands and doubled estimate of carbon storage. Nature Geoscience, 12: 917–921. DOI: 10.1038/s41561-019-0454-z

Ontario Geological Survey. 2011. Bedrock Geology of Ontario - Miscellaneous Release – Data 126 - Revision 1, scale 1:250 000.

Packalen MS, and Finkelstein SA. 2014. Quantifying Holocene variability in carbon uptake and release since peat initiation in the Hudson Bay Lowlands, Canada. Holocene, 24(9): 1063–1074. DOI: 10.1177/0959683614540728

Pellegrini AFA, Harden J, Georgiou K, Hemes KS, Malhotra A, Nolan CJ, et al. 2021. Fire effects on the persistence of soil organic matter and long-term carbon storage. Nature Geoscience, DOI: 10.1038/s41561-021-00867-1

Power MJ, Marlon JR, Bartlein PJ, and Harrison SP. 2010, Fire history and the Global Charcoal Database: A new tool for hypothesis testing and data exploration. Palaeogeography. Palaeoclimatology, Palaeoecology, 291(1): 52–59. DOI: 10.1016/j.palaeo.2009.09.014

Qiu C, Ciais P, Zhu D, Guenet B, Chang J, Chaudhary N, et al. 2022. A strong mitigation scenario maintains climate neutrality of northern peatlands. One Earth, 5(1): 86–97. DOI: 10.1016/j.oneear.2021.12.008

Qiu C, Zhu D, Ciais P, Guenet B, and Peng S. 2020. The role of northern peatlands in the global carbon cycle for the 21st century. Global Ecology and Biogeography, 29(5): 956–973. DOI: 10.1111/geb.13081

Reimer PJ, Austin WEN, Bard E, Bayliss A, Blackwell PG, Bronk Ramsey C, et al. 2020. The IntCal20 Northern Hemisphere Radiocarbon Age Calibration Curve (0–55 cal kBP). Radiocarbon, 62(4): 725–757. DOI: 10.1017/RDC.2020.41

Simard M, Lecomte N, Bergeron Y, Bernier PY, and Paré D. 2007. Forest productivity decline caused by successional paludification of boreal soils. Ecological Applications, 17(6): 1619–1637. PMID: 17913128 DOI: 10.1890/06-1795.1

Stocks BJ, Mason JA, Todd JB, Bosch EM, Wotton BM, Amiro BD, et al. 2002. Large forest fires in Canada, 1959–1997. Journal of Geophysical Research: Atmospheres, 107(D1): FFR 5-1–FFR 5-12. DOI: 10.1029/2001JD000484

Swindles GT, Morris PJ, Mullan DJ, Payne RJ, Roland TP, Amesbury MJ, et al. 2019. Widespread drying of European peatlands in recent centuries. Nature Geoscience, 12(11): 922–928. DOI: 10.1038/s41561-019-0462-z

Tam BY, Szeto K, Bonsal B, Flato G, Cannon AJ, and Rong R. 2019. CMIP5 drought projections in Canada based on the Standardized Precipitation Evapotranspiration Index. Canadian Water Resources Journal/Revue canadienne des ressources hydriques, 44(1): 90–107. DOI: 10.1080/07011784.2018.1537812

Turetsky M, Wieder K, Halsey L, and Vitt D. 2002, Current disturbance and the diminishing peatland carbon sink. Geophysical Research Letters, 29(11): 21-21–21-24. DOI: 10.1029/2001GL014000

Turetsky MR, Amiro BD, Bosch E, and Bhatti JS. 2004. Historical burn area in western Canadian peatlands and its relationship to fire weather indices. Global Biogeochemical Sciences, 17(4): GB4014, 4011-4019. DOI: 10.1029/2004GB002222

Turetsky MR, Benscoter B, Page S, Rein G, van der Werf GR, and Watts A. 2015. Global vulnerability of peatlands to fire and carbon loss. Nature Geoscience, 8(1): 11–14. DOI: 10.1038/ngeo2325

Turetsky MR, and Wieder RK. 2001. A direct approach to quantifying organic matter lost as a result of peatland wildfire. Canadian Journal of Forest Research-Revue Canadienne De Recherche Forestiere, 31(2): 363–366. DOI: 10.1139/x00-170

Turunen J, Tahvanainen T, Tolonen K, and Pitkänen A. 2001. Carbon accumulation in West Siberian Mires, Russia *Sphagnum* peatland distribution in North America and Eurasia during the past 21,000 years. Global Biogeochemical Cycles, 15(2): 285–296. DOI: 10.1029/2000GB001312

van Bellen S, Garneau M, Ali AA, and Bergeron Y. 2012. Did fires drive Holocene carbon sequestration in boreal ombrotrophic peatlands of eastern Canada?. Quaternary Research, 78(1): 50–59. DOI: 10.1016/j.yqres.2012.03.009

Vitt DH. 2006. Functional characteristics and indicators of boreal peatlands. *In* Boreal Peatland Ecosystems. *Edited by* RK Wieder and DH Vitt. Springer Berlin Heidelberg, Berlin, Heidelberg. p. 9–24.

Walker M, Gibbard P, Head MJ, Berkelhammer M, Björck S, Cheng H, et al. 2019. Formal subdivision of the Holocene Series/Epoch: A summary. Journal of the Geological Society of India, 93(2): 135–141. DOI: 10.1007/s12594-019-1141-9

Wang X, Parisien M-A, Taylor SW, Candau J-N, Stralberg D, Marshall GA, et al. 2017. Projected changes in daily fire spread across Canada over the next century. Environmental Research Letters, 12(2): 025005. DOI: 10.1088/1748-9326/aa5835

Wieder RK, Scott KD, Kamminga K, Vile MA, Vitt DH, Bone T, et al. 2009. Postfire carbon balance in boreal bogs of Alberta, Canada. Global Change Biology, 15(1): 63–81. DOI: 10.1111/j.1365-2486.2008.01756.x

Wilkinson SL, Moore PA, Thompson DK, Wotton BM, Hvenegaard S, Schroeder D, et al. 2018. The effects of black spruce fuel management on surface fuel condition and peat burn severity in an experimental fire. Canadian Journal of Forest Research, 48(12): 1433–1440. DOI: 10.1139/cjfr-2018-0217

Young DM, Baird AJ, Charman DJ, Evans CD, Gallego-Sala AV, Gill PJ, et al. 2019. Misinterpreting carbon accumulation rates in records from near-surface peat. Scientific Reports, 9(1): 17939. PMID: 31784556 DOI: 10.1038/s41598-019-53879-8

Young DM, Baird AJ, Gallego-Sala AV, and Loisel J. 2021. A cautionary tale about using the apparent carbon accumulation rate (aCAR) obtained from peat cores. Scientific Reports, 11(1): 9547. PMID: 33953225 DOI: 10.1038/s41598-021-88766-8

Yu ZC, Loisel J, Brosseau DP, Beilman DW, and Hunt SJ. 2010. Global peatland dynamics since the Last Glacial Maximum. Geophysical Research Letters, 37(5). DOI: 10.1029/2009GL042071

Zaccone C, Rein G, D'Orazio V, Hadden RM, Belcher CM, and Miano TM. 2014. Smouldering fire signatures in peat and their implications for palaeoenvironmental reconstructions. Geochimica et Cosmochimica Acta, 137: 134–146. DOI: 10.1016/j.gca.2014.04.018

Zoltai SC, Morrisset LA, Livingston GP, and de Groot WJ. 1998. Effects of fires on carbon cycling in North American boreal peatlands. Environmental Reviews, 6(1): 13–24. DOI: 10.1139/a98-002